SCIENCE CHINA
Information Sciences

• RESEARCH PAPER •

June 2022, Vol. 65 162402:1–162402:8
https://doi.org/10.1007/s11432-021-3286-3

Toward practical gas sensing with rapid recovery semiconducting carbon nanotube film sensors

Fangfang LIU[1†], Mengmeng XIAO[2*†], Yongkai NING[3†], Shaoyuan ZHOU[1], Jianping HE[1], Yanxia LIN[2] & Zhiyong ZHANG[1,2*]

[1]*Hunan Institute of Advanced Sensing and Information Technology, Xiangtan University, Xiangtan* 411105*, China;*
[2]*Key Laboratory for the Physics and Chemistry of Nanodevices and Center for Carbon-based Electronics, Department of Electronics, Peking University, Beijing* 100871*, China;*
[3]*Institute of Microelectronics of Chinese Academy of Sciences and University of Chinese Academy of Sciences, Beijing* 100029*, China*

Received 7 May 2021/Revised 12 June 2021/Accepted 22 June 2021/Published online 31 March 2022

Abstract Nanomaterials have been considered as promising materials to construct highly sensitive and miniaturized gas sensors due to their high ratio of surface to volume, but almost all of the reported nanomaterials based resistive gas sensors are difficult to use in the practical system mainly owing to the long recovery time and non-equilibrium state at room temperature. Here, we demonstrate a gate assistant technology to realize the rapid recovery to an equilibrium state in semiconducting carbon nanotube (CNT) thin-film gas sensors and promote the CNT-based gas sensors to reach the practical application level. Specifically, we construct highly uniform gas sensors based on semiconducting solution-derived CNT film and accelerate the gas molecules desorption by applying a voltage on the back gate (substrate), which is named gate-assistant recovery technology. By combining the gate-assistant recovery technology and a modified concentration calculation method, highly reproducible detection systems have been realized by using a custom-built printed circuit board (PCB) based data acquisition circuits to execute a real-time rapid detection of H_2 in the air at room temperature, and especially exhibits a record response time of 9 s and recovery time of 50 s under a resolution of 10 ppm, which outperformed previous low dimensional nanomaterials based portable H_2 detection systems. The gate-assistant rapid recovery and related concentration calculation technologies are helpful to promote the nanomaterials-based gas sensors to practical application for highly sensitive online gas detection.

Keywords carbon nanotube, gas sensor, thin-film transistors, rapid recovery

Citation Liu F F, Xiao M M, Ning Y K, et al. Toward practical gas sensing with rapid recovery semiconducting carbon nanotube film sensors. Sci China Inf Sci, 2022, 65(6): 162402, https://doi.org/10.1007/s11432-021-3286-3

1 Introduction

Modern gas sensors with high sensitivity, low power consumption, and a high level of integration are essential for safety and quality monitoring in various industrial processes [1–3]. Current mainstream commercial gas sensors based on resistive metal oxide semiconductors (MOS), which are in bulk and operated at a temperature higher than 200°C, are not favored in advanced gas sensing technology [4]. Recently, extensive investigations have been made on the use of atomically thin materials (ATMs) or named nanomaterials, including nanowires, nanotubes, and two-dimensional materials, to construct gas sensors with high sensitivity and high selectivity at room temperature, which provides a new opportunity to tackle those challenges of conventional gas sensors [5, 6]. Unfortunately, these ATMs gas sensors are usually far away from practical applications since they always suffer several critical defects, including poor reproduction and uniformity. The wafer-scale and uniform materials preparation and device fabrication, which are of great significance for the practical application, are still big challenges for most emerging ATMs sensors. More importantly, high affinity to the gas molecules in these ATMs leads to high sensitivity

* Corresponding author (email: mmxiao@pku.edu.cn, zyzhang@pku.edu.cn)
† Liu F F, Xiao M M, and Ning Y K have the same contribution to this work.

and rapid response on the one hand, but also results in long recovery time even to several hours at low operation temperature [7–9]. Furthermore, the combination of high affinity and large absorption capacitance due to the high surface-to-volume ratio of ATMs will bring a non-equilibrium response in practical time scale [10], and finally prevent the use of resistance response to evaluate the concentration in practical gas sensor systems [11, 12].

Carbon nanotube (CNT) has been considered as one of the promising ATMs for constructing highly sensitive chemical and bio-sensors owing to its unique structure, excellent electrical properties, and high stability [13,14]. CNT gas sensors with a batch fabrication ability in wafer-scale have been demonstrated for the room temperature detection of ppb level H_2 by utilizing high semiconducting purity solution-derived CNT films [15]. However, similar to other ATMs-based gas sensors, the reported CNT gas sensors still suffer from those challenges of long recovery time and non-equilibrium response. Some methods including UV light or on-chip heaters have been developed to accelerate the sensor recovery process, but these methods significantly increase the design/fabrication complexity and power consumption of the sensors [16, 17]. Therefore, it is necessary to develop a complete but simple scheme to promote the CNT gas sensors practically employed in the continuous online monitoring with fast recovery rate, appropriate concentration evaluation method, and wafer-scale batch fabrication ability.

In this work, we try to solute the major obstacles of ATM-based sensors and promote the CNT-based gas sensors to the practical application level. Specifically, we develop a gate assistant technology as well as improved data processing method to realize the rapid recovery in the CNT gas sensors, and the recovery time is as short as 50 s, which is more than an order of magnitude faster than natural recovery. Based on the highly uniform sensors fabricated on solution-derived semiconducting CNT network and decorated nanoparticles (NPs), highly reproducible detection systems have been realized by using custom-built printed circuit board (PCB)-based data acquisition circuits to execute a real-time rapid detection of H_2 in the air at room temperature. The gate-assistant rapid recovery and related concentration calculation technology are helping to promote the nanomaterials-based gas sensors to practical application for highly sensitive online gas detection.

2 Results and discussion

Back-gated thin-film-transistors (TFTs) were first fabricated based on highly uniform solution-derived CNT networks with high semiconducting purity through a well-developed micro-fabrication process [15, 18,19] (or see the fabrication details in Supporting information). Figures 1(a) and (b), respectively, show the UV-vis-NIR absorption and Raman spectroscopy of the CNT solutions. The invisible first metallic excitonic transitions peak (M11 between 600 and 800 nm in Figure 1(a)) and sharp S22 peak (820 –1350 nm) for CNT indicate an ultra-high semiconducting purity. The narrow RBM peak at 152 cm^{-1} in sorted CNT solution (Figure 1(b)) indicates a narrow diameter distribution around 1.6 nm according to the experimental relationship of $\omega = 248/d$ (nm). The fabricated sensors and their structural diagram are respectively shown in Figures 1(c) and (d). Statistical transfer curves of multiple pristine CNT TFTs (using Si substrate as a gate) shown in Figure 1(e) indicate an excellent electronic uniformity, which provides a good foundation to the uniform gas sensor platform. Three kinds of sensing materials, including 0.3 nm Pd/1 nm Au, 1 nm Sn (oxidized at 250°C for 30 min to form SnO_2), and 1 nm Pd, are deposited on the channels of different TFTs for the selective detection of H_2S, NO_2, and H_2, respectively [20–22]. Pt micro-heaters (Figure 1(c)) are also integrated with the gas sensor arrays on the same chip to study the heating assistance recovery effect. The scanning electron microscope (SEM) images in Figure 1(f) show that all the three sensing materials are well-dispersed as decoration NPs on the surface of the uniform network CNT film. The Raman spectrums before and after each sensing material modification were shown in Figure S1. To check the effect of different sensing NPs decoration, transfer characteristics of the CNT-TFTs measured before and after NPs decoration are shown in Figure 1(g). The decoration of semiconducting NPs such as SnO_2 leads to just a threshold voltage shift of CNT TFTs owing to the doping effect. However, the decoration of metallic NPs such as Pd or Pd/Au results in severe degradation on the current on/off ratio owing to the strong screening effect.

Transient responses of the functionalized CNT-TFTs for sensing H_2, H_2S, and NO_2 were characterized at room temperature in the air (see the detailed in Supporting information) as shown in Figure 2, in which each gas sensor was tested at two recovery conditions, i.e., a natural recovery and a gate assistant recovery by applying a gate voltage. Sensors were exposed to high-purity nitrogen before

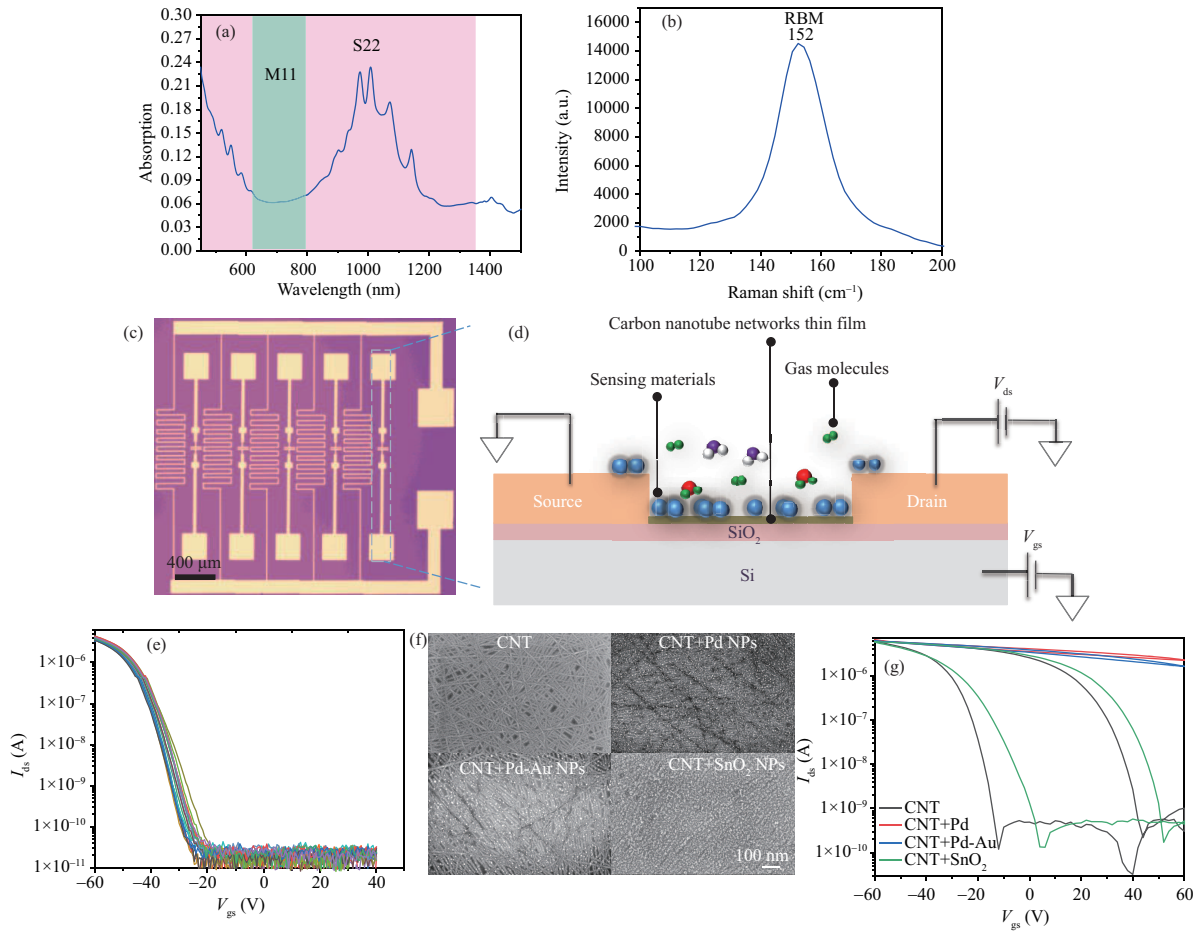

Figure 1 (Color online) Characteristics of CNT materials and structure and preliminary characteristics of CNT-TFT sensors. (a) Absorption spectrum and (b) Raman spectrum of the CNT solutions. (c) Optical microscope image of a multi-decorated CNT-TFT sensor array. (d) Cross-sectional schematic of a CNT-TFT sensor. (e) Statistical transfer curves of 17 CNT-TFTs at $V_{ds} = -1$ V using the substrate as a back gate. (f) SEM diagrams of CNT channels decorated without/with different sensing materials. Scale bar: 100 nm. (g) I_{ds}–V_{gs} curves of four devices measured with $V_{ds} = -1$ V in air. V_{gs} is swept from −60 to +60 V, then back to −60 V in a step of ±2 V.

measurements at each concentration to establish a baseline signal. The response of a sensor was defined as $S = (R - R_0)/R_0 = \Delta R/R_0$, where R_0 and R are the channel resistance before and after the target gas injection, respectively. The recovery time is simply defined as the time for the current resistance to recover to the original baseline of R_0. Figure 2(a) illustrates the response of a typical CNT-TFT sensor modified with 1 nm Pd to detect H_2 with a concentration range from 20 to 100 ppm and recovered naturally at room temperature. The response (S) begins to increase with the injection of H_2, and also begins to decline when H_2 flow was turned off as shown in Figure 2(a). The maximum response reaches up to 140% even for 20 ppm H_2, which indicates the high sensitivity. We also measured the selectivity of the Pd modified CNT film-based sensor to H_2, H_2S, and NO_2 as shown in Figure S2. However, the recovery time is longer than 300 s at natural recovery conditions and increases with the H_2 concentration. Especially after detecting 100 ppm H_2, the recovery time increases to 650 s, and such a long recovery time must severely hamper the real-time detection applications. The long recovery time of the gas sensors at room temperature is mainly owing to that the available thermal energy is usually much lower than the activation energy required in the desorption of hydrogen atoms in the NPs. When a gate assistant recovery condition is applied, i.e., a voltage of 60 V is applied on the back gate at the beginning of the recovery period, the response S shows fast recovery to the baseline in 50 s after the H_2 response as indicated by Figure 2(b). Moreover, we can use the same recovery time and voltage for the gas detection of different concentrations, which improves the simplicity in practical application. The three-terminal operation (using a back gate) for CNT-TFT-based gas sensors is attractive since it provides more flexible methods to manipulate the sensing performance with the gate voltage [23–25]. However, it still lacks the

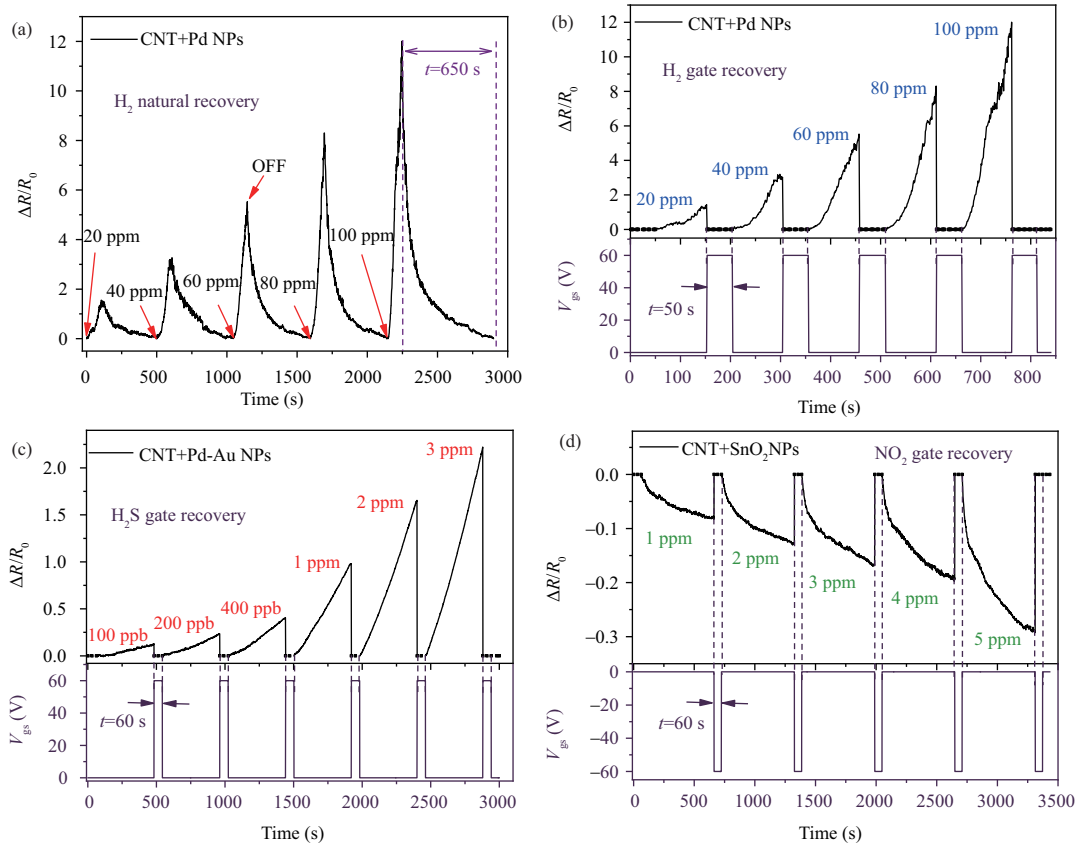

Figure 2 (Color online) Experimental characterizations of the transient response of the multi-functionalized CNT-TFT-based gas sensors under different recovery conditions. (a) The response of 1 nm Pd NPs-modified CNT-TFT device to different concentrations of H_2 gas at room temperature, and the device recovery time is up to 650 s after responding with 100 ppm H_2. (b) The response and recovery process of H_2 gas of different concentrations with gate assistant recovery and the recovery time is 50 s ($V_{gs} = +60$ V, $V_{ds} = -1$ V). (c) Rapid recovery test of H_2S gas at different concentrations with gate assistant recovery using CNT-TFT device modified with Pd 0.3 nm and Au 1 nm. The recovery time is 60 s ($V_{gs} = +60$ V, $V_{ds} = -1$ V). The response of the device to 100 ppb H_2S is 13%. (d) Rapid recovery test of NO_2 gas at different concentrations with gate assistant recovery using CNT-TFT device modified with SnO_2. The recovery time is 60 s ($V_{gs} = -60$ V, $V_{ds} = -1$ V).

study of applying the gate to realize fast recovery for the CNT-based gas sensors.

Response and recovery measurements were also performed in NO_2 and H_2S sensing and the results are shown in Figures 2(c) and (d). $Pd_{0.3nm}/Au_{1nm}$ NPs are used to decorate CNT-TFT gas sensors for the H_2S detection due to the strong and selective bonding energy of Au-S, and the sensors exhibit the detection limit lower than 100 ppb. However, with natural recovery in air, recovery time is as long as 720 s at 3 ppm. Under a gate assistant recovery condition, the recovery time declines to around 60 s for different concentrations H_2S by applying a back-gate voltage of +60 V. The sensitive and selective detection of NO_2 is achieved by SnO_2 decorated CNT-TFT sensors as shown in Figure 2(d). Different from electron donor molecules such as H_2 and H_2S, a negative gate voltage of −60 V was needed for the rapid recovery of the electron acceptor gas molecules such as NO_2 with a recovery time of 60 s. Benefited from the network morphology and ultra-thin semiconducting channel, the assistant gate voltage can provide an electric field to the NPs on the CNT film channel and then accelerates the desorption of target gas atoms or molecules by lowering the activation energy. Other methods such as heating-assistant recovery are widely used to accelerate desorption of gas atoms in gas sensing, but the gate assistant recovery method is more effective and more energy-saving (see the detailed comparison in Figure S3). Furthermore, the gate assistant recovery is a universal method for different gases to achieve rapid recovery of CNT-TFT-based gas sensors due to the thin body of the channel, either the CNT channel with or without hysteresis [26].

A common problem in nanomaterial sensors is the difficulty to establish an equilibrium state (or reach a plateau) in practical time scale since the current of the sensor is constantly changing until the sensor fails [10, 27, 28], which is also observed in all the three target gases sensing measurements using the modified CNT sensors. Through using the gate assistant technology, we can realize programmable CNT-

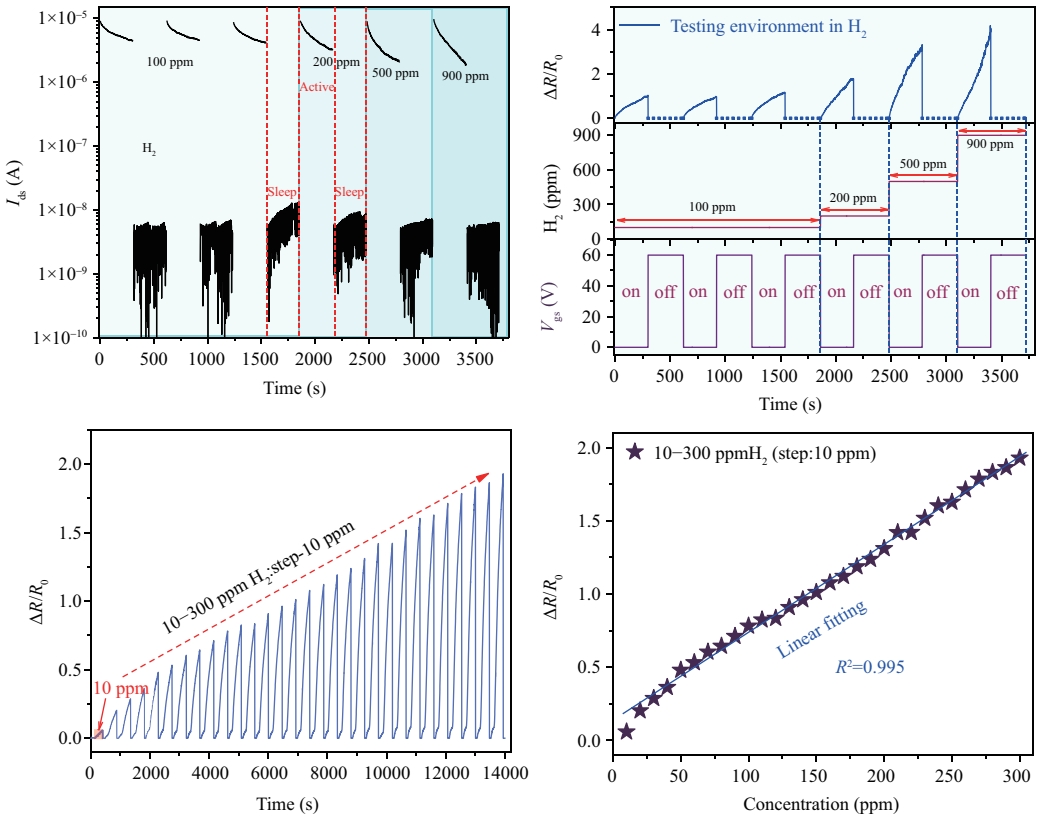

Figure 3 (Color online) Programmable control of the sensor response and H_2 testing in the actual environment. (a) The current changes of different concentrations of H_2 when the device is active (V_{gs} = 0 V) and sleep (V_{gs} = +60 V). (b) The corresponding response of (a). (c) The response of CNT-TFT modified with 1 nm Pd NPs to 30 H_2 concentration gradients (10–300 ppm, with 10 ppm intervals). (d) The relationship between final response values during active mode and H_2 concentration. The liner fitting (blue solid curve) has shown a good linear fitting coefficient of R^2 0.995.

TFT gas sensors to realize the control of the absorption and desorption of gas molecules by simply applying different back-gate voltages and refreshing the gas sensors periodically, thus avoiding the sensor failure. As shown in Figure 3(a), after the initialization stage in the air, H_2 with different concentrations carried by synthetic air were continuously injected into the test chamber to simulate the real-time monitoring of H_2 gas leakage. Under a gate bias of V_{gs} = 0 V, the sensor will be turned into the active mode and the continuous flow of H_2 will cause sustaining decline of the current. When a V_{gs} = +60 V is applied, the sensor was immediately turned into the sleep mode with an ultra-low standby current. The sensor at sleep mode is not responsive to H_2, and then can be well restored to the baseline with another zero-gate bias and ready for the next round of testing. With pulsed gate voltage applied as shown in the lower inset in Figure 3(b), the H_2 sensor was set alternately in the state of active or sleep with 300 s interval with four different H_2 concentrations. If there is a base concentration of target gas, the gas sensor will not output the sensing signal until they are under active mode. The gate-assistant programmable CNT-TFT gas sensors scheme will effectively lower the complexity of the subsequent control circuit in practical applications. It is worth mentioning that the voltage applied on the assistant gate is as high as tens of volts owing to the thick SiO_2 layer (500 nm) used in this work. However, it is possible to lower the assistant gate voltage to a few volts by using a local bottom gate with a thin insulator layer in the sensors.

The other key problem that originated from the non-equilibrium response in nanomaterials-based sensors is from accurately and rapidly evaluating the gas concentration in real-time [28, 29]. In a continuous monitoring case, the relative resistance change in the equilibrium state is widely used to evaluate the gas concentration in practical for the conventional resistive gas sensors. However, the concentration evaluation is impractical for the real-time continuous gas monitoring in nanomaterials-based gas in which the equilibrium state is hard to achieve [30–32]. In the gate assistant gas sensor, the concentration of the target gas can be retrieved according to the response speed (the slope in response-time representation) in the active mode. Figure 3(c) shows the dynamic test of the 1 nm Pd NPs modified CNT-TFT sensors to a series concentration of H_2 from 10 to 300 ppm with 10 ppm steps. In this process, the CNT gas sensor

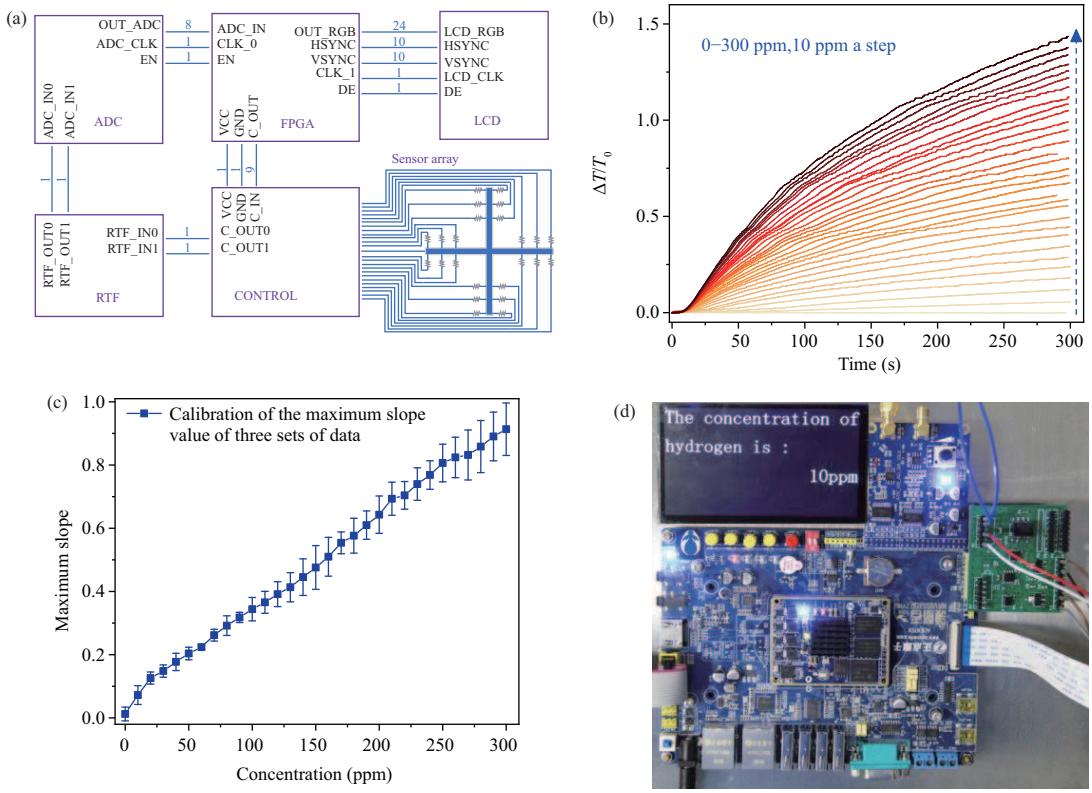

Figure 4 (Color online) Design of potable gas detection system and the H_2 detection in the actual environment. (a) Circuit schematic diagram of target gas detection system. (b) The relative change of RC oscillation period (ΔT) detected by the H_2 sensor system when 30 different concentrations of H_2 (0–300 ppm, step: 10 ppm) are successively injected, where ΔT is the difference between the RC oscillation period change before and after H_2 is injected. Assistant-gate recovery method is used with a recovery time of 50 s and recovery gate voltage $V_{gs} = +60$ V. (c) The calibration curve is performed by repeating the experiment three times (the oscillation period changes corresponding to 30 H_2 concentrations: 0–300 ppm, 10 ppm a step) and then taking the average value of the maximum slope. (d) The H_2 sensor detection system detects and displays H_2 with a resolution of 10 ppm.

is refreshed by the assistant gate and the relative response is strictly distinctive for each H_2 concentration with a resolution of 10 ppm. The relationship between different H_2 concentrations and their final response during the active mode is illustrated in Figure 3(d), which indicates that the linear correlativity between the response and H_2 concentration is very prominent with a liner coefficient R^2 of 0.995. The linear relationship will simplify the quantification of the concentration and cut down a lot of complex mathematical processing in real-time gas concentration monitoring applications.

To demonstrate the possibility of the practical application of our CNT TFT gas sensors, we built a PCB based data acquisition system for the real-time detection of the H_2 in the air at room temperature. The H_2 gas measurement system contains CNT-TFT sensors module, resistance-transfer-frequency (RTF) circuit module, control module, ADC (analog-to-digital converter) module, FPGA (field-programmable gate array) module, and screen display module, and the proposed circuit frame diagram is shown in Figure 4(a). The RTF block consists of a comparator and an operational amplifier, which converts the relative resistance change into relative RC oscillation period (T) change where $T \propto R$, as shown in Figure S4. The CNT-TFT gas sensors with RTF block were first characterized under different H_2 concentrations (0–300 ppm, with 10 ppm steps) with an oscilloscope. Each concertation was followed by an assistant gate recovery process to refresh the sensor sensing signal to the baseline. The relative oscillation period change over time is shown in Figure 4(b). Three repeated tests were conducted to show the repeatability and stability of our sensors as shown in Figures S5(a)–(c). The growth rate (slope) of each concentration is calculated by the differential of each response curve and the maximum slope can be reached in about 9 s as shown in Figures S6(a) and (b). Through three repeated tests, the average value of the maximum slope corresponding to each H_2 concentration is obtained as shown in Figure 4(c), which exhibits good linearity and uniformity. With such an evaluation process, the real-time monitoring of H_2 concentration is achieved as shown in Figure S7. We can evaluate the H_2 concentration accurately in less than 10 s by using the real-time slope of the response curve without waiting for the equilibrium

Table 1 Benchmark of H_2 sensor detection systems based on different nanomaterials[a)]

Channel material	Resolution	Response time	Recovery time	Test background	Reference
Pt-decorated SnO_2 nanotube	50 ppm	10 min	20 min	RT, air	[36]
Ni-Pd-decorated 3.5-nm-thin silicon	1%	∼2 s	No recovery (slowly)	RT, air	[37]
Pt-coated ZnO nanorods	200 ppm	∼5 min	15 min	RT, air	[38]
WO_3 and Pd bilayer	250 ppm	∼100 s	600 s	123°C, air	[39]
Pd/AlGaAs MOS HFET	15 ppm	∼1 h	3 h	RT, air	[40]
ZnO nanorods with Pd	10 ppm	∼5 min	15 min	RT, air	[41]
PdNi alloy thin films	10 ppm	∼10 min	75 min	50°C N_2	[42]
Pt-decorated rGO	1 ppm	12 s	60 s	RT, vacuum	[43]
Pd-decorated CNT thin film	10 ppm	9 s	50 s	RT, air	This work

a) RT: room temperature.

state as compared with the operation scheme in conventional resistive MOS sensors [33–35].

The period response data is then acquired by connecting the sensor/RTF module to an ADC and an FPGA module to analyze automatically the relative period change and to determine the real-time concentration by comparing the real-time slope with the stored calibration slope curve. Figure 4(d) indicates that our PCB based detection system can distinguish and display the H_2 leakage at a concentration of 10 ppm, which is consistent with the result measured by the oscilloscope, and the detection accuracy can reach 3.3% which is estimated as the ratio between resolution (10 ppm) and range (300 ppm). We then use a CNT-TFT-based custom-built PCB gas sensing system to continuously monitoring 10–100 ppm H_2 to confirm the reliability and repeatability of our sensing systems again as shown in Figure S8(a). With a smaller test chamber or larger gas flow, the response time can be further improved. Our H_2 system has shown a good resolution, a fast response time of less than 10 s as well as the shortest recovery time of 50 s at room temperature among the nanomaterials-based portable H_2 sensing systems (see Table 1 [36–43]). The CNT-TFT sensors with the assistant gate method can be used for real-time multi-point distribution detection of trace-level explosive and toxic gases and demonstrates the practical application potential as a portable gas sensor detection system.

3 Conclusion

In summary, we demonstrate a gate assistant technology to realize the rapid recovery to an equilibrium state in semiconducting CNT TFT gas sensors and promote the CNT-based gas sensors to reach the practical application level. Specifically, we construct highly uniform gas sensors based on semiconducting solution-derived CNT film and accelerate the gas molecules desorption by applying a voltage on the back gate. By combining the gate-assistant technology and an improved concentration calculation method, highly reproducible detection systems have been realized by using custom-built PCB based data acquisition circuits to execute a real-time rapid detection of H_2 in the air at room temperature, and especially exhibits a record response time of 9 s and recovery time of 50 s under a resolution of 10 ppm, which outperforms previous low dimensional nanomaterials based portable H_2 detection systems. The gate-assistant rapid recovery and related concentration calculation technologies are helpful to promote the nanomaterials-based gas sensors to practical application for highly sensitive online gas detection.

Acknowledgements This work was supported by the National Key Research & Development Program (Grant No. 2016YFA0201901). The authors thank Dr. Zhongqiu HUA from Peking University for the constructive discussions.

Supporting information Figures S1–S8. The supporting information is available online at info.scichina.com and link.springer.com. The supporting materials are published as submitted, without typesetting or editing. The responsibility for scientific accuracy and content remains entirely with the authors.

References

1 Ponnuvelu D V, Dhakshinamoorthy J, Prasad A K, et al. Geometrically controlled Au-decorated ZnO heterojunction nanostructures for NO_2 detection. ACS Appl Nano Mater, 2020, 3: 5898–5909
2 Arshak K, Moore E, Lyons G M, et al. A review of gas sensors employed in electronic nose applications. Sens Rev, 2004, 24: 181–198
3 Nazemi H, Joseph A, Park J, et al. Advanced micro- and nano-gas sensor technology: a review. Sensors, 2019, 19: 1285
4 Kim H J, Lee J H. Highly sensitive and selective gas sensors using p-type oxide semiconductors: overview. Sens Actuat B-Chem, 2014, 192: 607–627
5 Yuan W J, Shi G Q. Graphene-based gas sensors. J Mater Chem A, 2013, 1: 10078
6 Kauffman D R, Star A. Carbon nanotube gas and vapor sensors. Angew Chem Int Ed, 2008, 47: 6550–6570

7 Zhang M, Brooks L L, Chartuprayoon N, et al. Palladium/single-walled carbon nanotube back-to-back Schottky contact-based hydrogen sensors and their sensing mechanism. ACS Appl Mater Interface, 2014, 6: 319–326
8 Zhang T, Nix M B, Yoo B Y, et al. Electrochemically functionalized single-walled carbon nanotube gas sensor. Electroanalysis, 2006, 18: 1153–1158
9 Star A, Joshi V, Skarupo S, et al. Gas sensor array based on metal-decorated carbon nanotubes. J Phys Chem B, 2006, 110: 21014–21020
10 Kumar D, Chaturvedi P, Saho P, et al. Effect of single wall carbon nanotube networks on gas sensor response and detection limit. Sens Actuat B-Chem, 2017, 240: 1134–1140
11 Ding D Y, Chen Z, Rajaputra S, et al. Hydrogen sensors based on aligned carbon nanotubes in an anodic aluminum oxide template with palladium as a top electrode. Sens Actuat B-Chem, 2007, 124: 12–17
12 Li Y X, Li G H, Wang X W, et al. Poly(ionic liquid)-wrapped single-walled carbon nanotubes for sub-ppb detection of CO_2. Chem Commun, 2012, 48: 8222
13 Liang Y Q, Xiao M M, Wu D, et al. Wafer-scale uniform carbon nanotube transistors for ultrasensitive and label-free detection of disease biomarkers. ACS Nano, 2020, 14: 8866–8874
14 Schroeder V, Savagatrup S, He M, et al. Carbon nanotube chemical sensors. Chem Rev, 2019, 119: 599–663
15 Xiao M M, Liang S B, Han J, et al. Batch fabrication of ultrasensitive carbon nanotube hydrogen sensors with sub-ppm detection limit. ACS Sens, 2018, 3: 749–756
16 Li J, Lu Y J, Ye Q, et al. Carbon nanotube sensors for gas and organic vapor detection. Nano Lett, 2003, 3: 929–933
17 Robinson J A, Snow E S, Badescu S C, et al. Role of defects in single-walled carbon nanotube chemical sensors. Nano Lett, 2006, 8: 1747–1751
18 Samanta S K, Fritsch M, Scherf U, et al. Conjugated polymer-assisted dispersion of single-wall carbon nanotubes: the power of polymer wrapping. Acc Chem Res, 2014, 47: 2446–2456
19 Homenick C M, Rousina-Webb A, Cheng F, et al. High-yield, single-step separation of metallic and semiconducting SWCNTs using block copolymers at low temperatures. J Phys Chem C, 2014, 118: 16156–16164
20 Geng J, Thomas M D R, Shephard D S, et al. Suppressed electron hopping in a Au nanoparticle/H_2S system: development towards a H_2S nanosensor. Chem Commun, 2005, 65: 1895
21 Maiti A, Rodriguez J A, Law M, et al. SnO_2 nanoribbons as NO_2 sensors: insights from first principles calculations. Nano Lett, 2003, 3: 1025–1028
22 Tian J W, Jiang H C, Zhao X H, et al. A Ppb-level hydrogen sensor based on activated Pd nanoparticles loaded on oxidized nickel foam. Sens Actuat B-Chem, 2021, 329: 129194
23 Fan Z Y, Lu J G. Gate-refreshable nanowire chemical sensors. Appl Phys Lett, 2005, 86: 123510
24 Peng N, Zhang Q, Lee Y C, et al. Gate modulation in carbon nanotube field effect transistors-based NH_3 gas sensors. Sens Actuat B-Chem, 2008, 132: 191–195
25 Tong Y, Lin Z H, Thong J T L, et al. MoS_2 oxygen sensor with gate voltage stress induced performance enhancement. Appl Phys Lett, 2015, 107: 123105
26 Ervin M H, Dorsey A M, Salaets N M. Hysteresis contributions to the apparent gate pulse refreshing of carbon nanotube based sensors. Nanotechnology, 2009, 20: 345503
27 He Q Y, Zeng Z Y, Yin Z Y, et al. Fabrication of flexible MoS_2 thin-film transistor arrays for practical gas-sensing applications. Small, 2012, 8: 2994–2999
28 Liu Y M, Yu J C, Cui Y, et al. An AC sensing scheme for minimal baseline drift and fast recovery on graphene FET gas sensor. In: Proceedings of International Conference on Solid-state Sensors, 2017. 230–233
29 Yuan Z, Bariya M, Fahad H M, et al. Trace-level, multi-gas detection for food quality assessment based on decorated silicon transistor arrays. Adv Mater, 2020, 32: 1908385
30 Nallon E C, Schnee V P, Bright C, et al. Chemical discrimination with an unmodified graphene chemical sensor. ACS Sens, 2016, 1: 26–31
31 Kumar R, Jenjeti R N, Sampath S. Two-dimensional, few-layer $MnPS_3$ for selective NO_2 gas sensing under ambient conditions. ACS Sens, 2020, 5: 404–411
32 Jang D, Jung G, Jeong Y, et al. Efficient integration of si FET-type gas sensors and barometric pressure sensors on the same substrate. In: Proceedings of IEEE International Electron Devices Meeting, 2019. 630–633
33 Fine G F, Cavanagh L M, Afonja A, et al. Metal oxide semiconductor gas sensors in environmental monitoring. Sensors-Basel, 2010, 6: 5469–5502
34 Kumar R, Zheng W, Liu X H, et al. MoS_2 based nanomaterials for room temperature gas sensors. Adv Mater Technol, 2020, 5: 1901062
35 Wang C X, Yin L W, Zhang L Y, et al. Metal oxide gas sensors: sensitivity and influencing factors. Sensors, 2010, 10: 2088–2106
36 Chen J Q, Chen Z, Boussaid F, et al. Ultra-low-power smart electronic nose system based on three-dimensional tin oxide nanotube arrays. ACS Nano, 2018, 6: 6079–6088
37 Fahad H M, Shiraki H, Amani M, et al. Room temperature multiplexed gas sensing using chemical-sensitive 3.5-nm-thin silicon transistors. Sci Adv, 2017, 3: 1602557
38 Huang Y S, Chen Y Y, Wu T T. A passive wireless hydrogen surface acoustic wave sensor based on Pt-coated ZnO nanorods. Nanotechnology, 2010, 21: 095503
39 Jakubik W P. Hydrogen gas-sensing with bilayer structures of WO_3 and Pd in SAW and electric systems. Thin Solid Films, 2009, 517: 6188–6191
40 Hsu C S, Lin K W, Chen H I, et al. On a heterostructure field-effect transistor (HFET) based hydrogen sensing system. Int J Hydrogen Energy, 2011, 36: 15906–15912
41 Jun J, Chou B, Lin J, et al. A hydrogen leakage detection system using self-powered wireless hydrogen sensor nodes. Solid-State Electron, 2007, 51: 1018–1022
42 Jiang H C, Tian X Y, Deng X W, et al. Low concentration response hydrogen sensors based on wheatstone bridge. Sensors-Basel, 2019, 5: 1096
43 Lee J S, Oh J, Jun J, et al. Wireless hydrogen smart sensor based on Pt/graphene-immobilized radio-frequency identification tag. ACS Nano, 2015, 9: 7783–7790